REPORT DOCUMENTATION PAGE

AFRL-SR-AR-TR-04-

0289

1. AGENCY USE ONLY *(Leave blank)*	2. REPORT DATE	3. REPORT TYPE AND DATES COVERED
	Final	15 Oct 03 - 14 Mar 04

4. TITLE AND SUBTITLE
MISAR: Waveform Design and Filtering in Zak Space

5. FUNDING NUMBERS
FA9550-04-C-0003

6. AUTHOR(S)
Richard Tolimieri
Myoung An

7. PERFORMING ORGANIZATION NAME(S) AND ADDRESS(ES)
Prometheus, Inc.
103 Mansfield Street
Sharon, MA 02067

8. PERFORMING ORGANIZATION REPORT NUMBER

9. SPONSORING/MONITORING AGENCY NAME(S) AND ADDRESS(ES)
Air Force Office Of Scientific Research
4015 Wilson Blvd., Room 713
Arlington, VA 22203-1954

DM

10. SPONSORING/MONITORING AGENCY REPORT NUMBER

11. SUPPLEMENTARY NOTES

12a. DISTRIBUTION AVAILABILITY STATEMENT
Distribution Statement A: Approved for Public Release; Distribution Unlimited

12b. DISTRIBUTION CODE

13. ABSTRACT *(Maximum 200 words)*

In this report, we document our ongoing effort to develop the Finite Zak Transform (FZT) into a framework for adaptive signal and filter design. The general idea is that by representing one-dimensional signals in multi-dimensional spaces, the underlying geometry in these multi-dimensional spaces can lead to new signal decompositions and processing methods. The specific application outlined in this report is spatial localization and scattering co-effiecient computation from the noisy echos of chirp waveforms interrogating a point target environment. The methods developed will be extended in future efforts to materials identification from chirp pulse echoes including the determination of the scattering delays due to dielectric materials. Numerical experiments are included to emphasize the feasibility of this approach Zak space representation provides a geometric, time-frequency setting for developing tools for solving this problem. In this setting we have established: geometric conditions for choosing optimal or nearly optimal sampling rates for the echoes of the chirp waveforms, methods for processing and interpreting the information contained in the resulting sampled echoes.

14. SUBJECT TERMS

15. NUMBER OF PAGES
31

16. PRICE CODE

17. SECURITY CLASSIFICATION OF REPORT	18. SECURITY CLASSIFICATION OF THIS PAGE	19. SECURITY CLASSIFICATION OF ABSTRACT	20. LIMITATION OF ABSTRACT
U	U	U	SAR

Final Report

2 June 2004

Sponsored by
Air Force Office of Scientific Research
USAF, AFRL

Contract # FA9550-04-C-0003

Contractor: Prometheus Inc.
Business Address: 103 Mansfield Street, Sharon, MA 02067

Effective Date of Contract: 15 October 2003
Contract Expiration Date: 15 April 2004
Reporting Period: 15 October 2003 – 2 June 2004

Principal Investigator: Richard Tolimieri
Phone Number: (401) 849-5389, (781) 784-2355
Title: MISAR: Waveform Design and Filtering in Zak Space
Authors: Richard Tolimieri, Myoung An

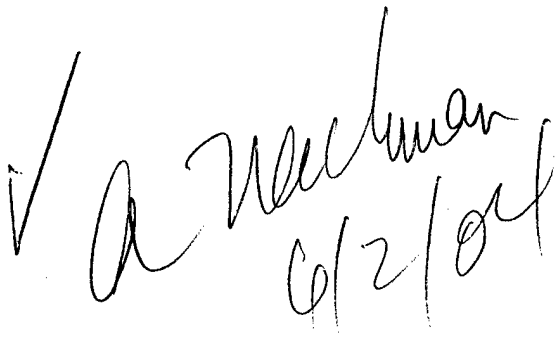

Disclaimer

Distribution Requirement

1 Introduction

In this report we document our ongoing effort to develop the finite Zak transform (FZT) into a framework for adaptive signal and filter design. The general idea is that by representing one-dimensional signals in multi-dimensional spaces, the underlying geometry in these multi-dimensional spaces can lead to new signal decompositions and processing methods.

The specific application outlined in this report is *spatial localization* and *scattering coefficient* computation from the noisy echoes of chirp waveforms interrogating a point target environment. The methods developed will be extended in future efforts to materials identification from chirp pulse echoes including the determination of the scattering delays due to dielectric materials. Numerical experiments are included to emphasize the feasibility of this approach.

Zak space representation provides a geometric, time-frequency setting for developing tools for solving this problem. In this setting we have established

- geometric conditions for choosing optimal or nearly optimal sampling rates for the echoes of the chirp waveforms,
- methods for processing and interpreting the information contained in the resulting sampled echoes.

In general the FZT of a sampled chirp pulse is not an (algebraic) line, copies of a line or even sparsely supported. However, we have identified a collection of appropriate sampling rates for a chirp pulse, depending on chirp rate, carrier frequency and time duration. The resulting sampled chirps are said to satisfy a Zak space condition. The FZT of these sampled chirps consist of copies of a line.

Throughout this report results will be shown for sampled chirps satisfying a Zak space condition. Similar results continue to hold for sample rates any integer multiple of those identified and, more generally, whenever Zak space representations are sparsely supported. These extensions are critical for increasing target resolution and will be a subject of future efforts.

The FZT of a cyclic shift of a sampled chirp pulse satisfying a Zak space condition also consists of lines. Under certain nonsingularity conditions the supports of the FZT of two sufficiently closely spaced cyclic shifts are disjoint. A (mathematical) echo formed from linear combinations of closely spaced cyclic shifts can be analyzed by decomposing the FZT of the echo into the disjoint lines corresponding to these cyclic shifts. If the shifts are not closely spaced then standard methods are applicable.

A main result is that under certain nonsingularity conditions, the collection of cyclic shifts of a sampled chirp pulse satisfying a Zak space condition is orthogonal. As a consequence any (mathematical) echo can be resolved by matched filtering or inner product computations.

In general matched filtering is optimum in the presence of white noise for resolving echoes formed by shifts of arbitrary waveforms. However the FZT of an echo formed by cyclic shifts of a sampled chirp satisfying a Zak space condition has predictable geometric structure. The support of the echo is the union of lines and these lines are all shifts of a known line. Noise

reduction in Zak space involves detecting these lines in noise and, in extreme conditions, reconstructing the lines from partial lines, rotated lines or otherwise corrupted lines.

Image processing methods in the Zak domain for denoising and focusing are under development. A two-step procedure of detection of lines and partial lines using abelian group filters, followed by filtering in the image domain, has been implemented. More advanced noncommutative group filters are being tested to detect rotated and other corrupted lines.

For applications, beginning with section 3, we extend results on cyclic shifts to linear shifts of zero-padded chirps. The main change, a consequence of the matrix form of the uncertainty principle, is that blurring factors are introduced. The collection of all linear shifts is no longer orthogonal. However, in section 6 we determine certain orthogonal collections of linear shifts.

Zak domain representation provides a space for viewing an echo from different perspectives not directly available in the usual time-domain or frequency-domain representations. In this report we investigate the effect of Zak domain windowing and filtering on the detailed analysis of echoes from transmitted chirps.

Two general issues will be addressed. First, a collection of non-orthogonal linear shifts when viewed over a proper Zak space window becomes an orthogonal collection. In general windowing results in information loss but for special target scenarios we can, by windowing, replace an echo formed by a linear combination of non-orthogonal shifts by a windowed echo consisting of a linear combination of orthogonal windowed shifts, without information loss.

Windowing is most effective for target scenes consisting of several clusters of closely spaced targets which are sufficiently separated. Specifics as to what is meant by closely spaced and sufficiently separated will be indicated in the following sections. Windowing results in *local* orthogonality. If the clusters are sufficiently separated the local orthogonality results in *global* orthogonality and the methods of the previous report can be applied.

More advanced Zak space filtering operations will be introduced for focusing in on local regions of a target scene. The problem is not completely solved in this report but these techniques completely solve the focusing problem under certain assumptions of the target scene. Generally if the target clusters are not too close then standard methods as well as Zak space methods can be used to localize the problem.

The goal is to combine Zak space windowing and filtering operations with multiple chirp interrogations for the purpose of designing robust and computationally efficient algorithms for resolving a general point target scene. One of the most important consequences of multiple chirp rates is that the scene can be investigated at different sample rates and viewed through different Zak space representations.

Although details of the derivation of the Zak space filtering algorithm are somewhat complex the resulting algorithm is robust in the presence of noise, has simple implementation and is more computationally efficient as compared with the standard approach.

2 Zak Space Conditions

Suppose $N = LK$ and $M = \frac{K}{L}$, where N is the number of chirp samples. Certain conditions called *Zak space conditions* on the discrete chirp

$$x(n) = e^{\pi i a\left(\frac{n}{L}\right)^2} e^{2\pi i b \frac{n}{L}}, \quad n \in \mathbf{Z},$$

have been defined. The $L \times K$ FZT of a discrete chirp satisfying the $L \times K$ Zak space condition consists of a finite number of copies of an algebraic line. The $L \times K$ FZT of a zero-padded discrete chirp is discussed in section 4.

For a vector $\mathbf{x}$ in $\mathbf{C}^N$,

$$\mathbf{x} = \begin{bmatrix} x_0 \\ x_1 \\ \vdots \\ x_{N-1} \end{bmatrix}, \quad x_n \in \mathbf{C},\ 0 \le n < N,$$

form the $L \times K$ matrix $M_L\mathbf{x}$ whose k-th column is

$$\begin{bmatrix} x_k \\ x_{k+K} \\ \cdot \\ \cdot \\ \cdot \\ x_{k+(L-1)K} \end{bmatrix}, \quad 0 \le k < K.$$

The $L \times K$ FZT of $\mathbf{x}$ is the $L \times K$ matrix $Z_L\mathbf{x}$ whose k-th column is

$$X_k = F(L) \begin{bmatrix} x_k \\ x_{k+K} \\ \cdot \\ \cdot \\ \cdot \\ x_{k+(L-1)K} \end{bmatrix}, \quad 0 \le k < K,$$

where $F(L)$ is the $L \times L$ Fourier transform matrix

$$F(L) = \left[v^{jk}\right]_{0 \le j,\, k < L}, \quad v = e^{2\pi i \frac{1}{L}}.$$

We have

$$Z_L\mathbf{x} = [X_0\, X_1 \cdots X_{K-1}] = F(L) M_L\mathbf{x}.$$

Since

$$M_L\mathbf{x} = F(L)^{-1} Z_L\mathbf{x},$$

$\mathbf{x}$ and $Z_L\mathbf{x}$ contain equivalent information. The $L \times K$ FZT presents a two-dimensional $L \times K$ time-frequency image of $\mathbf{x}$, called the $L \times K$ *Zak space representation* of $\mathbf{x}$. Different

factorizations of N lead to different Zak space representations, each depicting different time-frequency properties of $\mathbf{x}$. For example, if $L = 1$, $Z_L\mathbf{x}$ is the transpose of $\mathbf{x}$. In this case the Zak space representation is the signal itself. If $L = N$, $Z_L\mathbf{x}$ is the N-point Fourier transform of $\mathbf{x}$. Zak transforms for $L = 1$, $L = N$ and $1 < L < N$, where $N = 384$, are displayed in Figures 2.1 – 2.3.

Figure 2.1. Discrete chirp : Zak transform of dimension $L = 1$

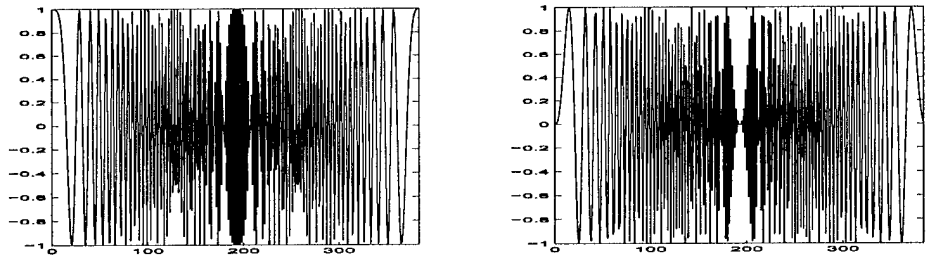

Real part Imaginary part

Sampled analog chirp with $\gamma = .0938$, $\beta = 0.0$, $T = 64$.

Figure 2.2. Fourier transform of discrete chirp: Zak transform of dimension $L = N$

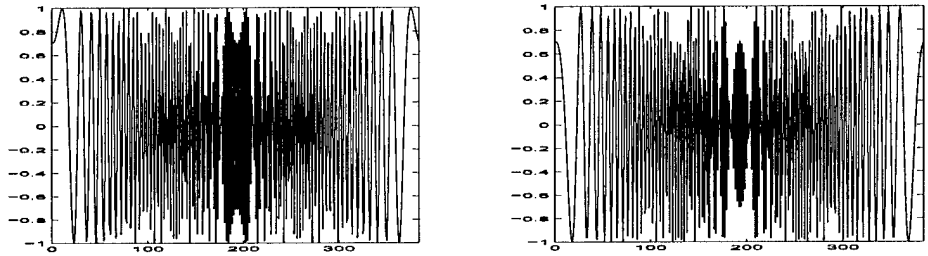

Real part Imaginary part

Figure 2.3. Zak transform of dimension $L \times K = 16 \times 24$

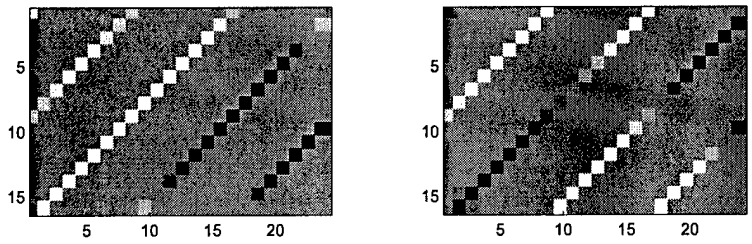

Real part Imaginary part

In the following sections we will study nonsingular discrete chirps satisfying the $L \times K$ Zak space condition and their cyclic shifts and extensions to zero-padded discrete chirps and their linear shifts. Results will lead to algorithms for analyzing echoes formed from linear shifts.

What appears to be essential is the sparseness of the Zak space representations of these signals and their shifts, which imposes for closely spaced shifts disjointness in their Zak space representation supports and in general *some* degree of orthogonality for arbitrary shifts. Since Z_L is a linear isomorphism, and up to scale multiple, an isometry, it is reasonable to determine the class of all discrete chirps and more generally classes of discrete signals having sparse Zak space representations and study the extent to which properties holding for the discrete chirps in this report continue to hold for these other classes of signals. This information can then be applied to increase flexibility in sampling rates and target resolution. This study is now underway.

Discrete chirp signals satisfying the $L \times K$ Zak space condition and their Zak transforms are displayed in Figures 2.4 – 2.11.

Figure 2.4. Discrete chirp and its Zak transform

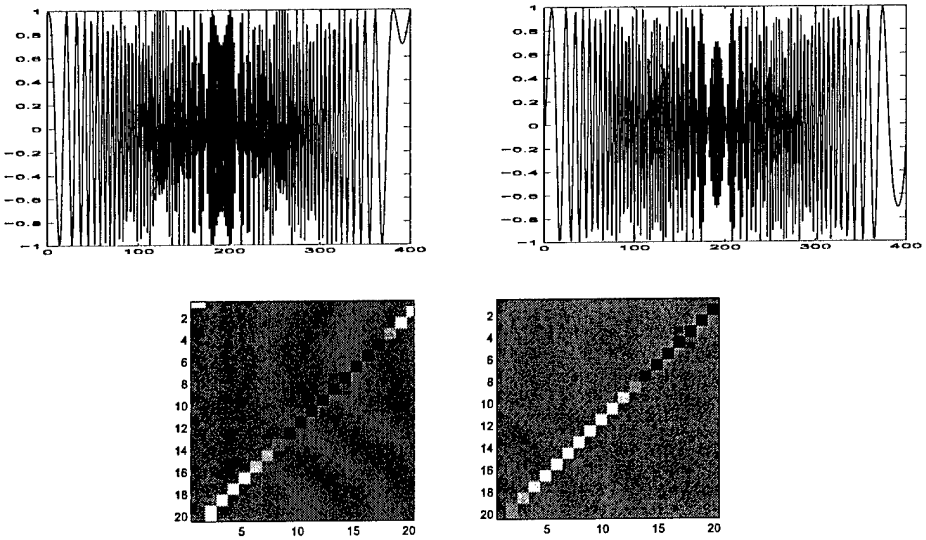

Real part Imaginary part

The discrete chirp corresponds to the sampled analog chirp with $\gamma = .44$, $\beta = .33$, $T = 30.0$. It satisfies the 20×20 Zak space condition with $M = 1$, $a = 1$, $b = \frac{1}{2}$.

Figure 2.5. Discrete chirp and its Zak transform

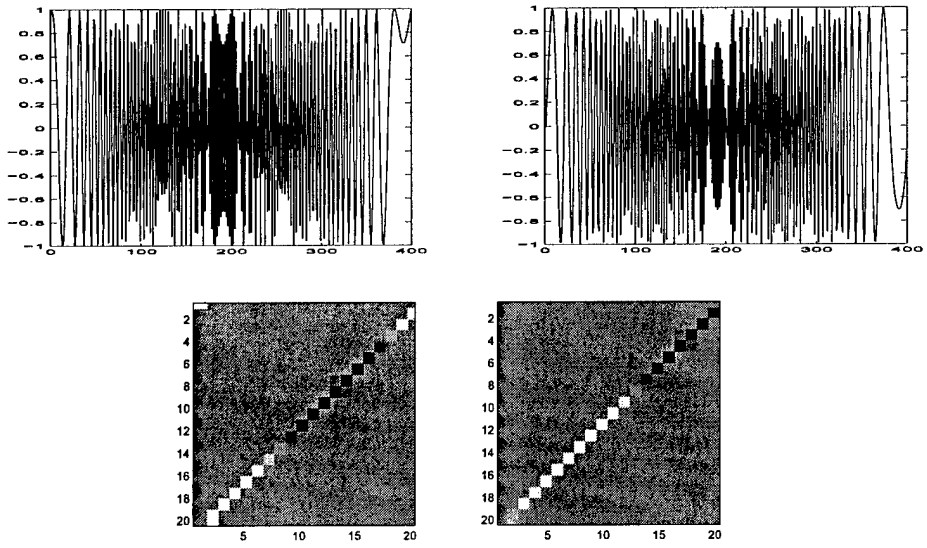

Real part Imaginary part

The discrete chirp corresponds to the sampled analog chirp with $\gamma = .44$, $\beta = 67$, $T = 30.0$. It satisfies the 20×20 Zak space condition with $M = 1$, $a = 1$, $b = 100\frac{1}{2}$.

Figure 2.6. Discrete chirp and its Zak transform

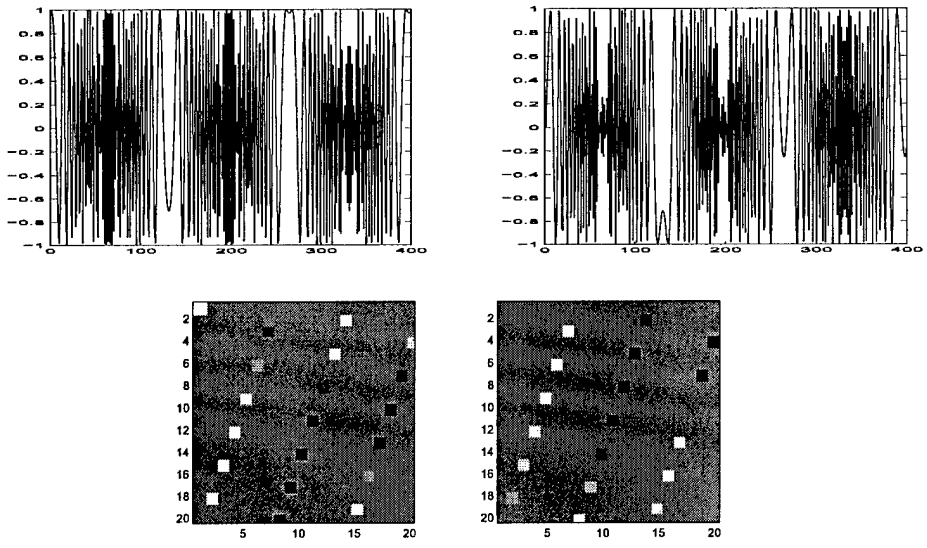

Real part Imaginary part

The discrete chirp corresponds to the sampled analog chirp with $\gamma = 1.33$, $\beta = .33$, $T = 30.0$. It satisfies the 20×20 Zak space condition with $M = 1$, $a = 3$, $b = \frac{1}{2}$.

Figure 2.7. Zak transform of a discrete chirp: $M = 1$, even case

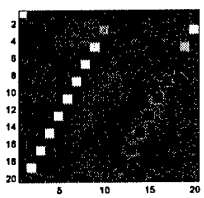
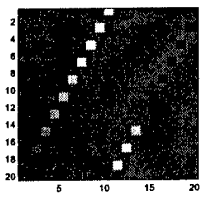
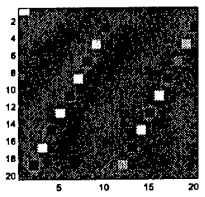
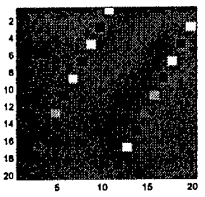

Real Imaginary Real Imaginary

$a = 2 \leftrightarrow \gamma = .88$, $b = 0 \leftrightarrow \beta = 0$ $a = 2 \leftrightarrow \gamma = .88$, $b = 20 \leftrightarrow \beta = 20$

Figure 2.8. Zak transform of a discrete chirp: $M = 1$, odd case

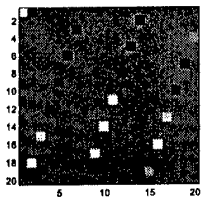
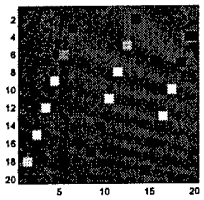
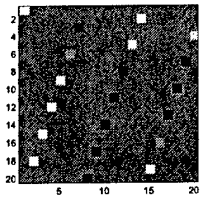
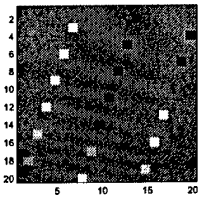

Real Imaginary Real Imaginary

$a = 3 \leftrightarrow \gamma = 1.33$, $b = 1.5 \leftrightarrow \beta = 1$ $a = 3 \leftrightarrow \gamma = 1.33$, $b = 100.5 \leftrightarrow \beta = 67$

Figure 2.9. Zak transform of a discrete chirp: $M = 2$, even cases

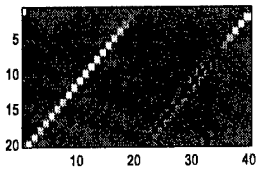
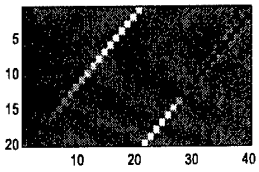
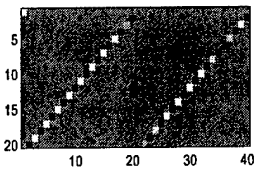
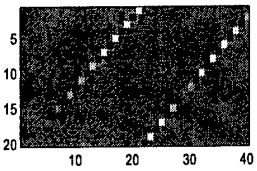

Real Imaginary Real Imaginary

$a = .5 \leftrightarrow \gamma = .88$, $b = 0 \leftrightarrow \beta = 0$ $a = .5 \leftrightarrow \gamma = .88$, $b = 90 \leftrightarrow \beta = 120$

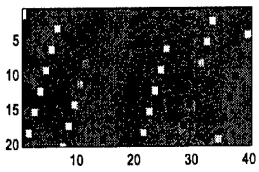
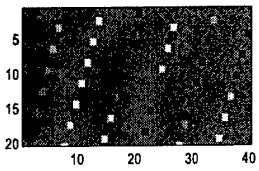
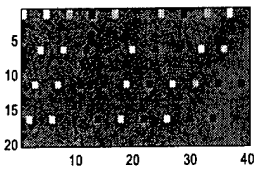
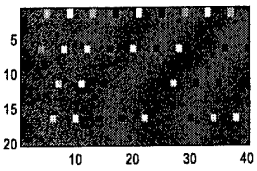

Real Imaginary Real Imaginary

$a = 1.5 \leftrightarrow \gamma = 2.66$, $b = 0 \leftrightarrow \beta = 0$ $a = 2.5 \leftrightarrow \gamma = 4.44$, $b = 0 \leftrightarrow \beta = 0$

Figure 2.10. Zak transform of a discrete chirp: $M = \frac{1}{2}$, even case

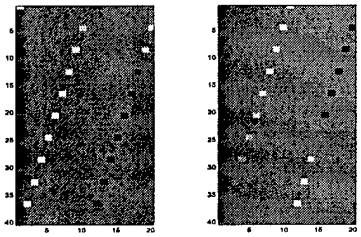

Real Imaginary

$a = 8 \leftrightarrow \gamma = 3.55,\ b = 0 \leftrightarrow \beta = 0$

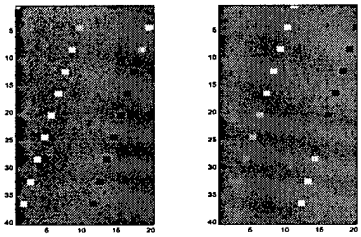

Real Imaginary

$a = 8 \leftrightarrow \gamma = 3.55,\ b = 120 \leftrightarrow \beta = 80$

Figure 2.11. Zak transform of a discrete chirp: $M = \frac{1}{2}$, odd case

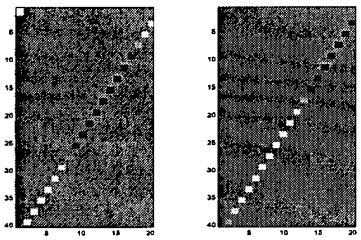

Real Imaginary

$a = 4 \leftrightarrow \gamma = 1.77,\ b = .66 \leftrightarrow \beta = 0$

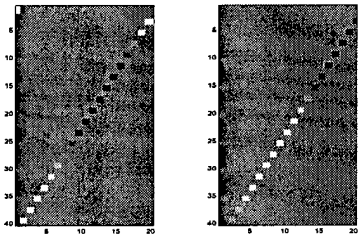

Real Imaginary

$a = 4 \leftrightarrow \gamma = 1.77,\ b = 80.66 \leftrightarrow \beta = 80$

3 Cyclic Shifts

In this section we study the cyclic shifts of a nonsingular discrete chirp x satisfying the $L \times K$ Zak space condition. The main result shows that if x satisfies an *extended* nonsingularity condition, then the collection of all its cyclic shifts is an orthogonal set.

As discussed, these methods and computations can be described without reference to Zak space. The design of the discrete chirp is critical to their applicability by these methods.

In Figures 3.1 and 3.2, Zak transforms of a chirp satisfying the Zak space condition and some of its shifts are displayed. Images in Figure 3.3 are superpositions of the results of the Zak transforms, illustrating the disjoint supports.

Figure 3.1. Zak transforms of a chirp and its shifts

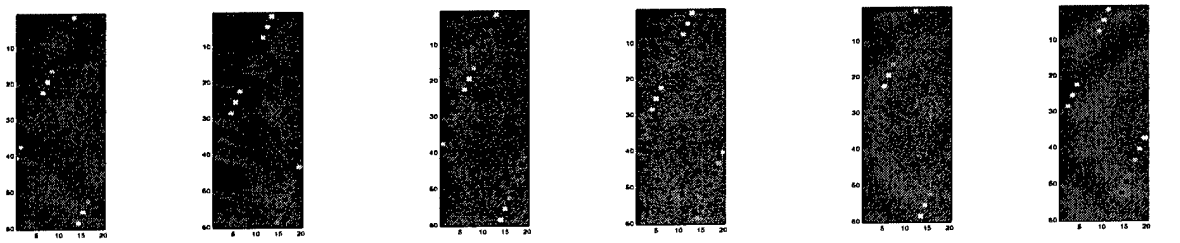

Real Imaginary Real Imaginary Real Imaginary

$K = 20$, $L = 60$, $a = 9$,$b = 50.5$. shift by 1 shift by 2

Figure 3.2. Zak transforms of a chirp and its shifts

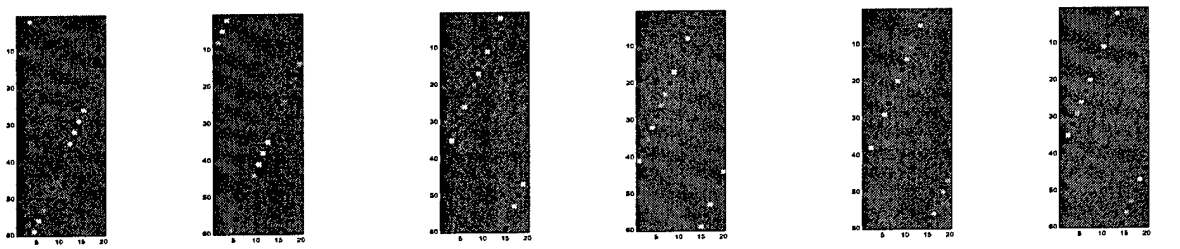

Real Imaginary Real Imaginary Real Imaginary

shift by 10 shift by 200 shift by 1000

Figure 3.3. Superpositions of Zak transforms and shifts

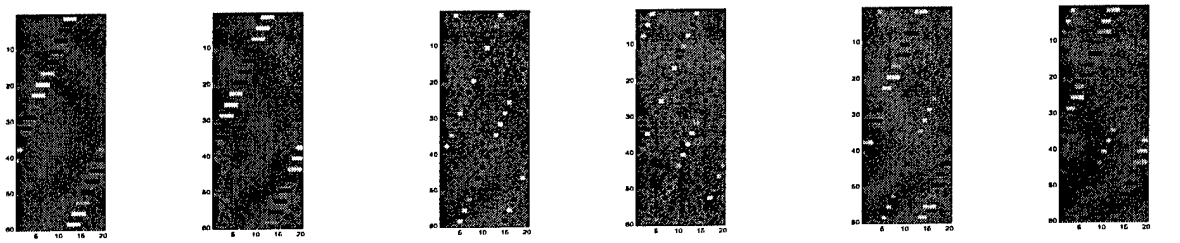

Real Imaginary Real Imaginary Real Imaginary

first set second set both sets

Figures 3.4 – 3.19 illustrate the performance of image processing in the Zak domain. Our first implementation consists of two distinct procedures, detection and location of lines using abelian group filters, and filtering in the image domain using the location for denoising. Several refinements are under development, including the use of noise characteristics. Once the location of lines is determined, the background (everything other than targets) will be characterized as noise. We will investigate methods of using this adaptive characterization to improve signal information.

Locating and denoising a cyclically shifted discrete chirp in Zak space is illustrated in Figures 3.4 – 3.8. In Figures 3.4 – 3.6 and 3.9, values of only the first 10 of 40 nanoseconds are displayed. Each sample interval corresponds to 0.0694 nanoseconds.

Figure 3.4. Discrete chirp: $a = 1$, $b = .5$, $T = 40$, $L \times K = 24 \times 24$.

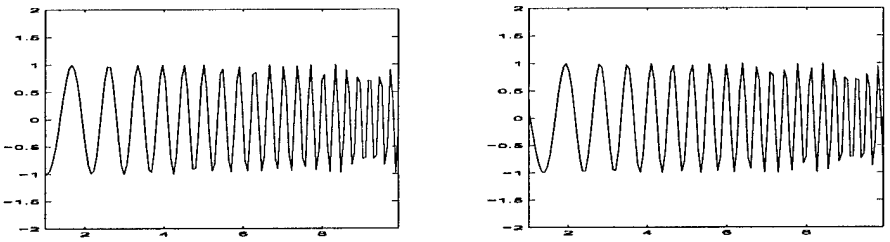

Real Imaginary

Figure 3.5. Cyclically shifted discrete chirp: Shift by 5 sample intervals.

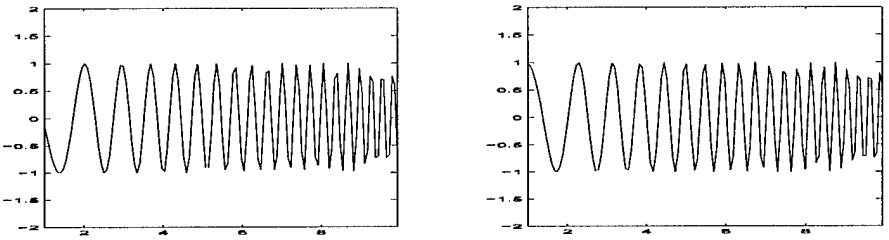

Real Imaginary

Figure 3.6. Cyclically shifted noisy discrete chirp.

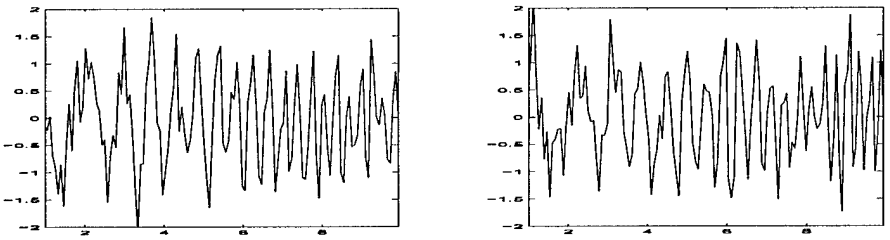

Real Imaginary

Figure 3.7. dB plot of the signal-to-noise ratio.

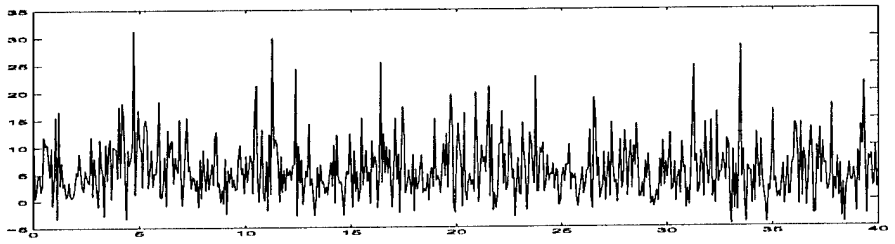

Figure 3.8. Zak transform of the noisy, shifted discrete chirp.

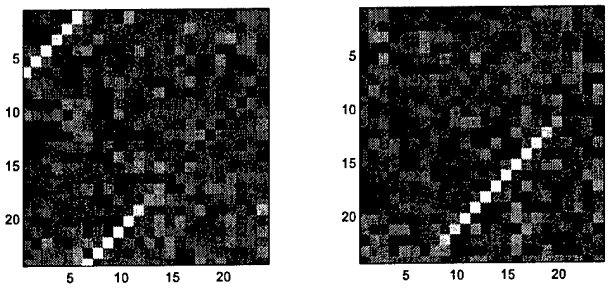

Figure 3.9. Result of applying image processing.

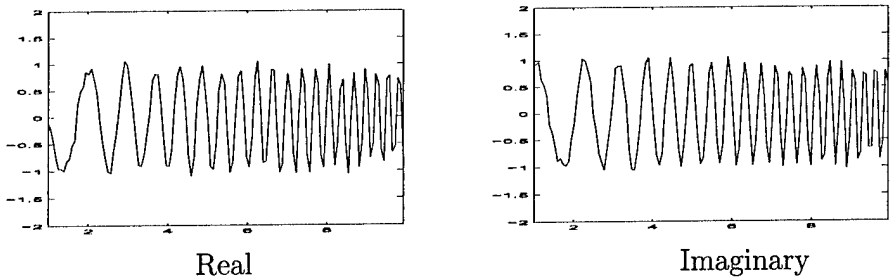

Resolving, locating and denoising multiple, cyclically shifted discrete chirps in Zak space are illustrated in Figures 3.10 – 3.14. In Figures 3.10, 3.11 and 3.14, values of only the first 10 of 40 nanoseconds are displayed. Each sample interval corresponds to 0.0694 nanoseconds.

Figure 3.10. Sum of two cyclically shifted discrete chirps: Shifts by 4 and 9 sample intervals.

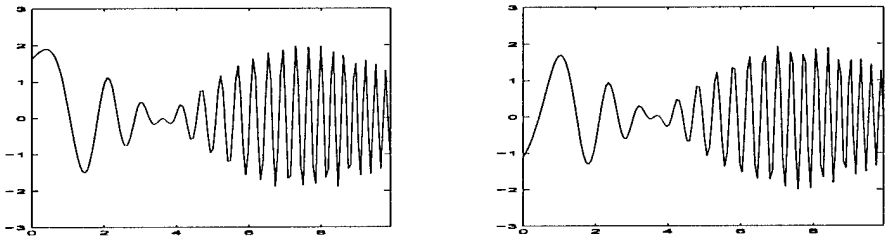

Real Imaginary

Figure 3.11. Sum of two noisy, shifted discrete chirps.

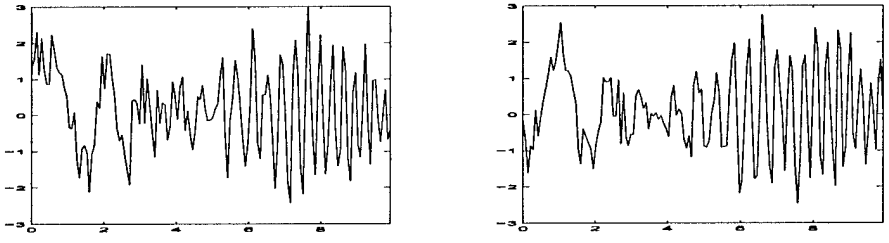

Real Imaginary

Figure 3.12. dB plot of the signal-to-noise ratio.

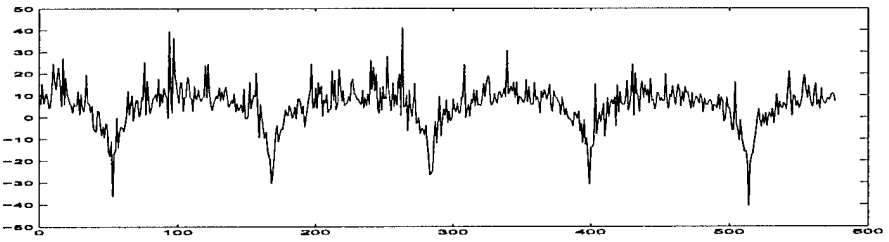

Figure 3.13. Zak transform of the sum of two noisy, shifted discrete chirps.

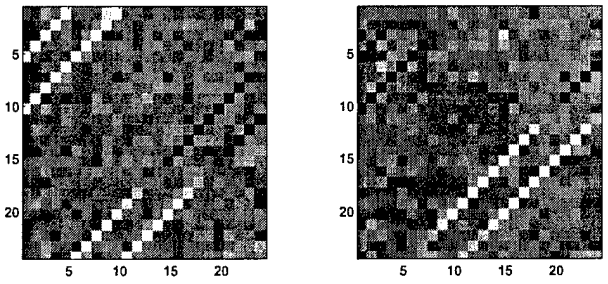

Real Imaginary

The result of the first procedure in the image processing algorithm consists of two numbers, indicating two detections and their positions. The number of targets is not required as an input for this procedure. The second procedure uses the position information to filter out the noise in the Zak domain.

Figure 3.14. Results of image filtering and Zak transform inversion.

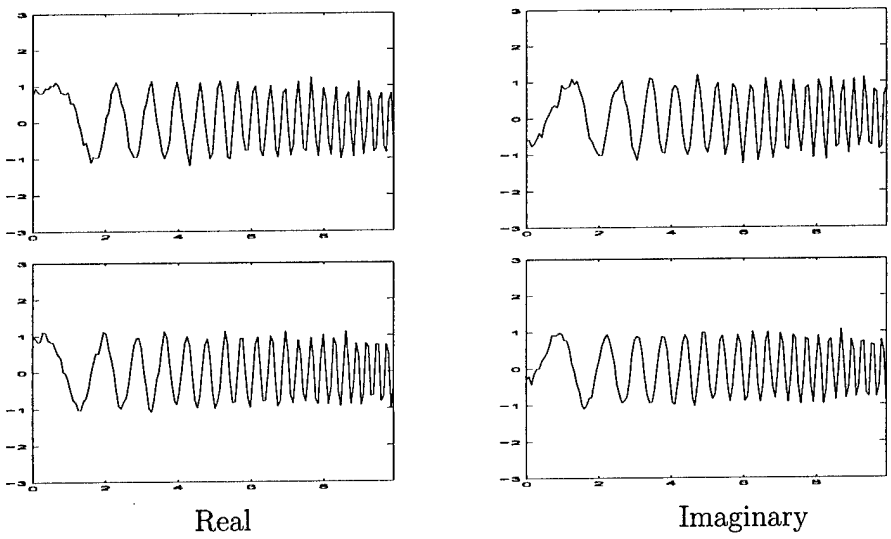

Real Imaginary

Figure 3.15. Sum of three cyclically shifted discrete chirps: Shifts by 2, 4 and 11 samples.

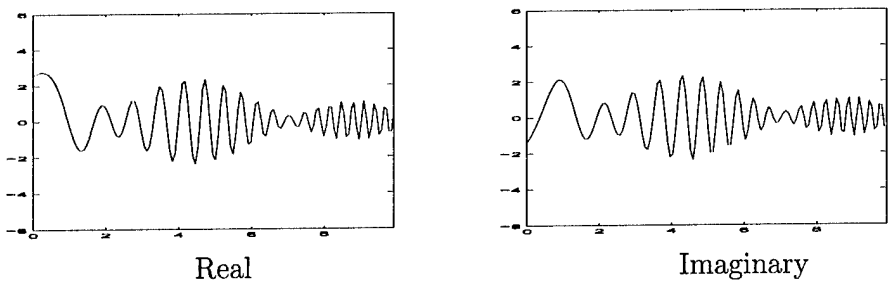

Real Imaginary

Figure 3.16. Sum of three noisy, shifted discrete chirps.

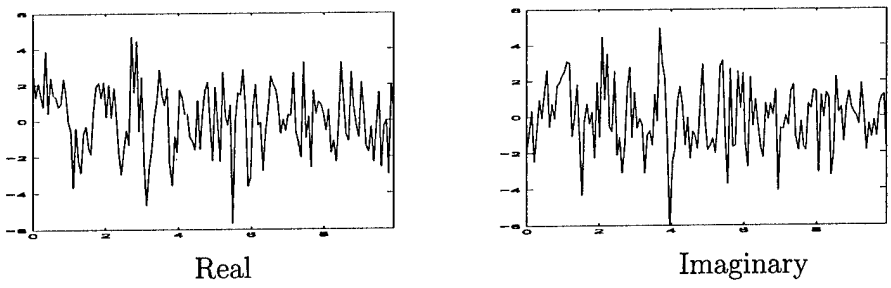

Real Imaginary

Figure 3.17. dB plot of the signal-to-noise ratio.

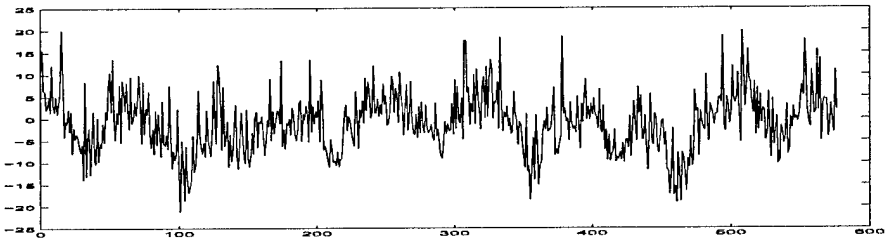

Figure 3.18. Zak transform of the sum of three noisy, shifted discrete chirps.

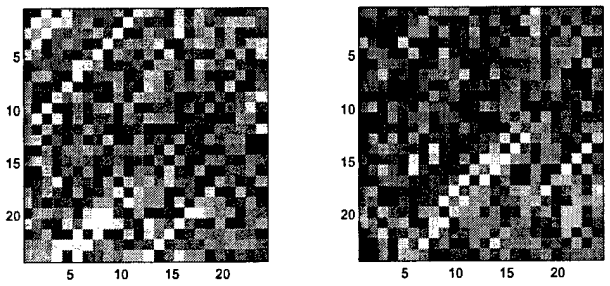

Real Imaginary

The result of the first procedure in the image processing algorithm consists of two numbers, indicating two detections and their positions. Thus, the software failed to detect/locate the third target. The second procedure uses the position information to filter out the noise in the Zak domain.

Figure 3.19. Results of image filtering and Zak transform inversion.

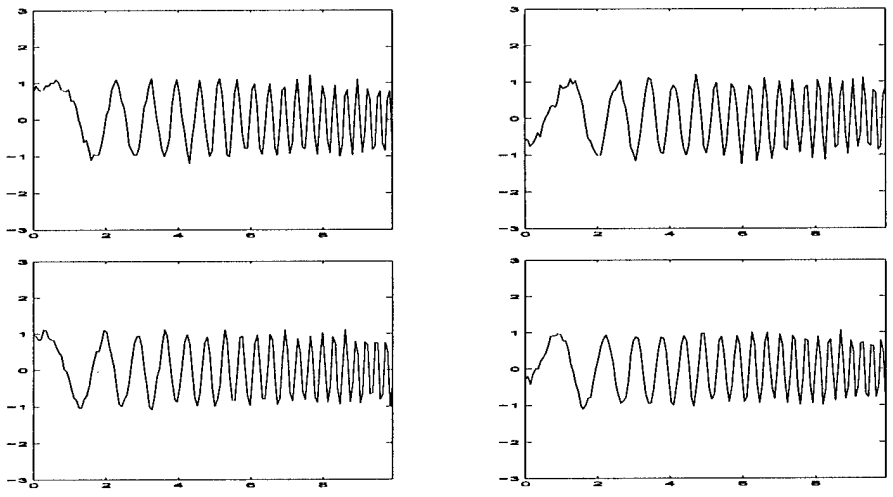

Real Imaginary

4 FZT of Zero-padded Chirps

For applications the results of the preceding two sections must be extended to linear rather than cyclic shifts. This goal is accomplished by defining a permuted Zak transform.

The first pair of images in Figure 4.1 displays the Zak transform of a zero-padded, discrete chirp satisfying the Zak space condition, while the second pair displays the corresponding permuted Zak transform, $P(RL, R)Z_{RL}\mathbf{x}^R$. The pair of images in Figure 4.2 displays the first L rows of $P(RL, R)Z_{RL}\mathbf{x}^R$.

Figure 4.1. Zak transform of zero-padded chirps

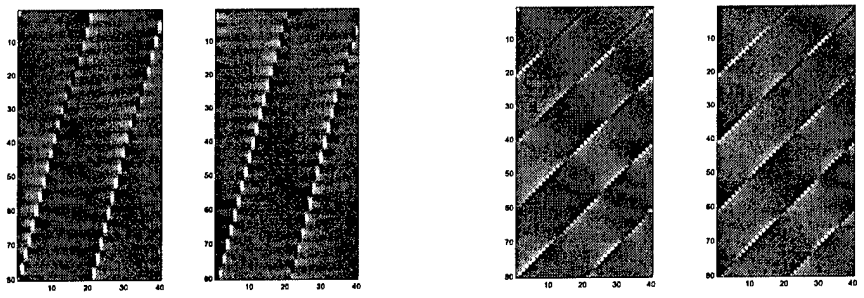

Real Imaginary Real Imaginary

$R = 4$, $K = 40$, $L = 20$, $a = .5$,$b = .5$. Permuted Zak transform

Figure 4.2. Zak transform of zero-padded chirps: first L rows

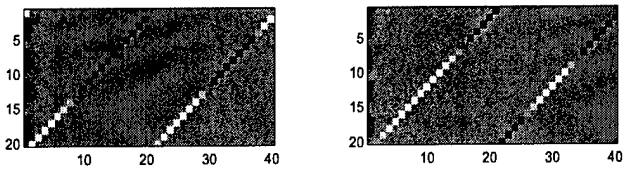

Real Imaginary

Permuted Zak transform

Figures 4.3 – 4.6 display Zak transforms and permuted Zak transforms of zero-padded chirps for varying parameters, R, K and L. In all cases the chirp parameters are determined to satisfy the $L \times K$ Zak space conditions.

Figure 4.3. Zak transform of zero-padded chirp

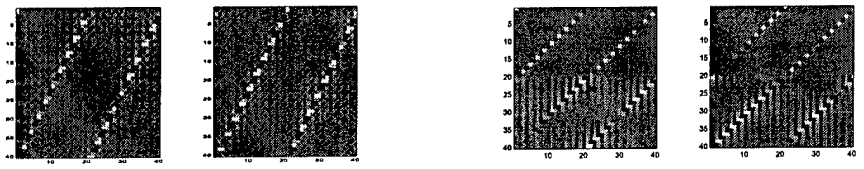

Real Imaginary Real Imaginary

$R = 3$, $K = 40$, $L = 20$, $a = .5$,$b = 50$. Permuted Zak transform

Figure 4.4. Zak transform of zero-padded chirp

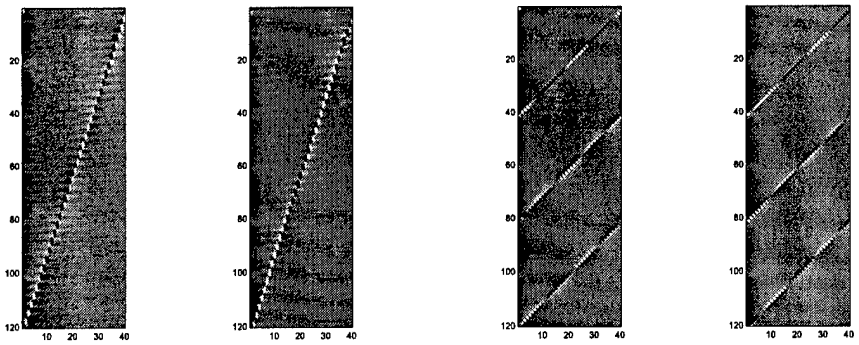

Real Imaginary Real Imaginary

$R = 3$, $K = 40$, $L = 40$, $a = 1$,$b = 121.5$. Permuted Zak transform

Figure 4.5. Zak transform of zero-padded chirp

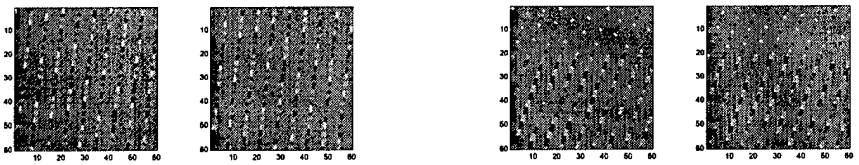

Real Imaginary Real Imaginary

$R = 3$, $K = 60$, $L = 20$, $a = 1$,$b = 50.5$. Permuted Zak transform

Figure 4.6. Zak transform of zero-padded chirp

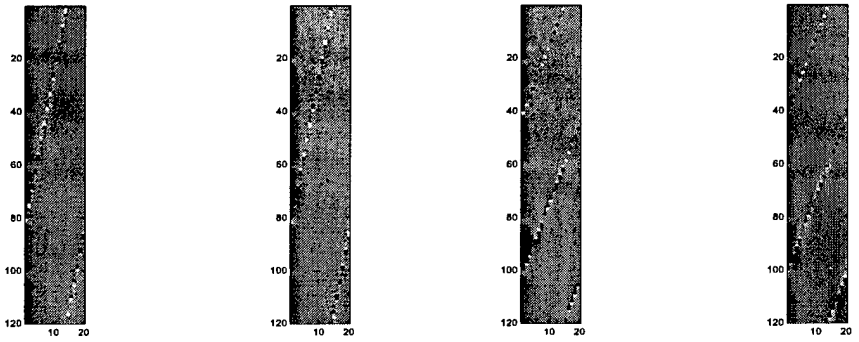

Real Imaginary Real Imaginary

$R = 2$, $K = 20$, $L = 60$, $a = 9$,$b = 50.5$. Permuted Zak transform

Zak domain image processing for denoising zero-padded discrete chirps is also accomplished. The result of the image processing is displayed in Figure 4.9.

Figure 4.7. Zero-padded discrete chirp.

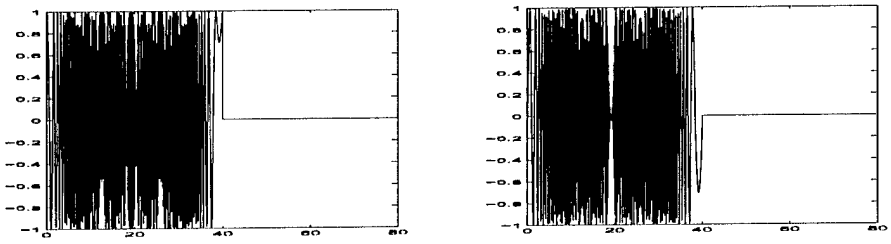

Real Imaginary

Figure 4.8. Noisy, zero-padded discrete chirp.

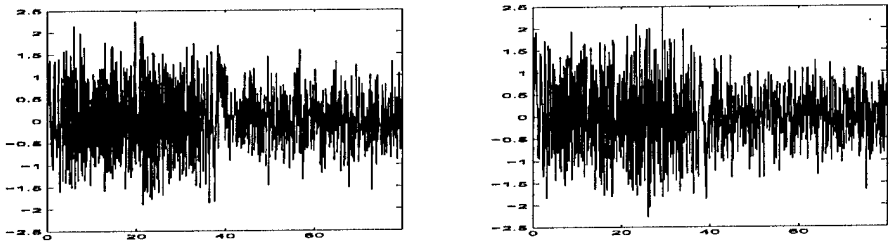

Real Imaginary

Figure 4.9. Result of image processing in Zak domain.

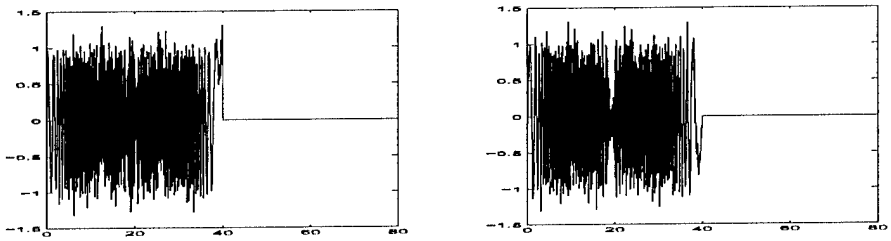

Real Imaginary

5 Linear Shifts

Resolving two linearly shifted (delayed) discrete chirps in Zak space is illustrated in Figures 5.1 – 5.3. Such resolution in the presence of noise is illustrated in Figures 5.4 – 5.6. The two linear shifts are resolved in the Zak space, but with ambiguity up to the parameter L. In these figures, the first shift is by $129 \equiv 4 \, mod \, 25$ and the second shift is by $133 \equiv 8 \, mod \, 25$.

Figure 5.1. Linearly shifted discrete chirps: $a = 1$, $b = .5$, $T = 40$, $L \times K = 25 \times 25$, $R = 2$.

Shift by 129 sample intervals

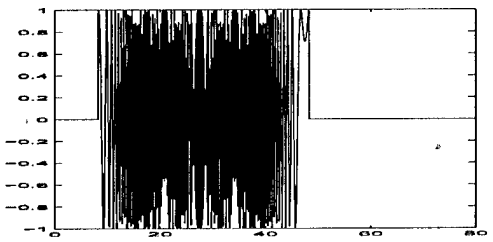

Real

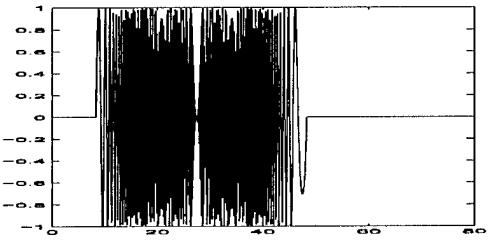

Imaginary

Shift by 133 sample intervals.

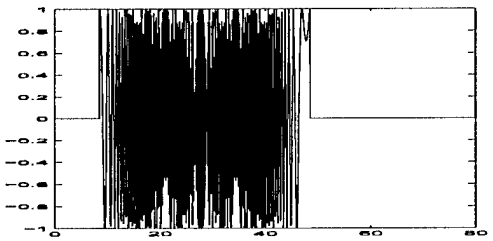

Real

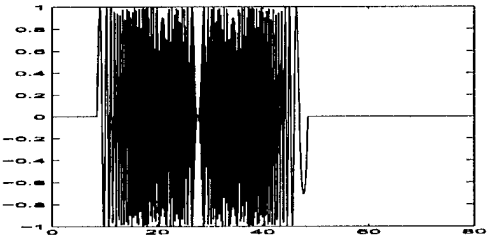

Imaginary

Figure 5.2. Sum of two shifted discrete chirps.

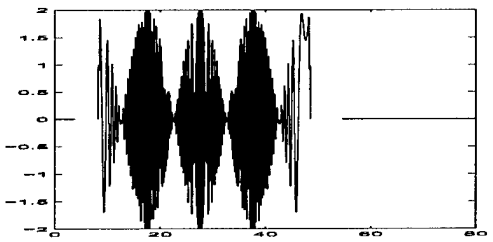

Real

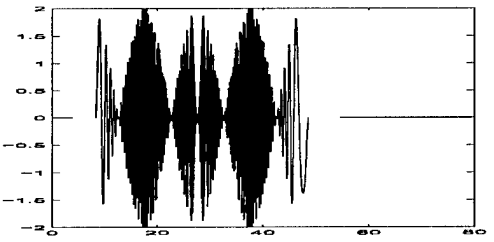

Imaginary

Figure 5.3. Zak transform of the sum of two shifted discrete chirps.

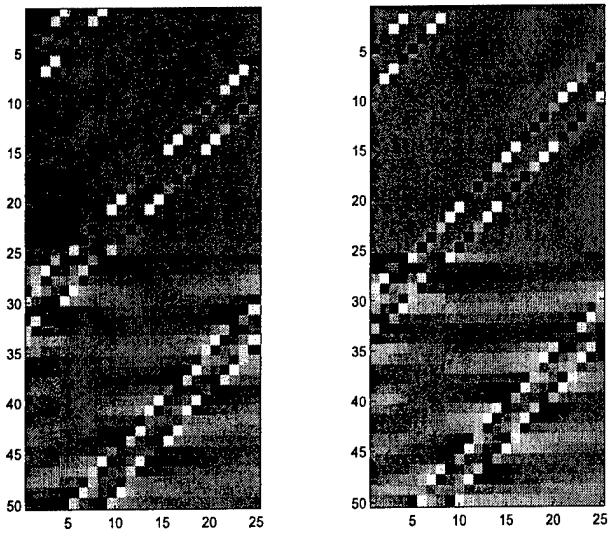

Figure 5.4. Linearly shifted discrete chirps with additive noise.
$a = 1$, $b = .5$, $T = 40$, $L \times K = 25 \times 25$, $R = 2$.

Shift by 125 sample intervals

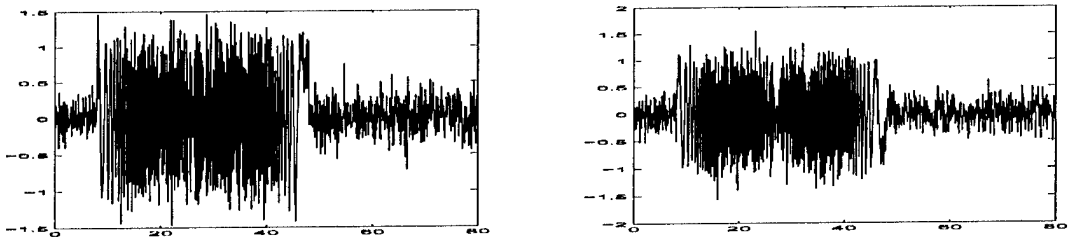

Shift by 133 sample intervals.

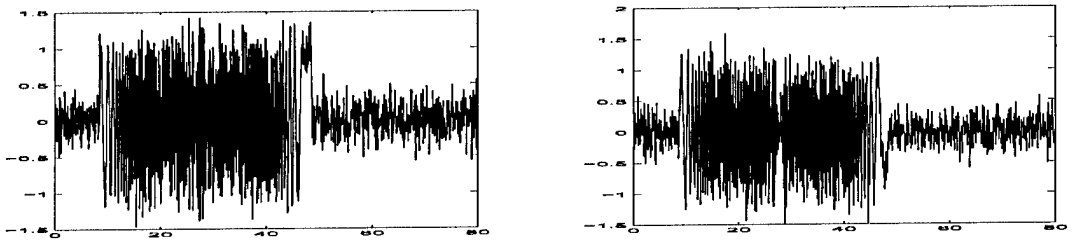

Figure 5.5. Sum of two shifted, noisy discrete chirps.

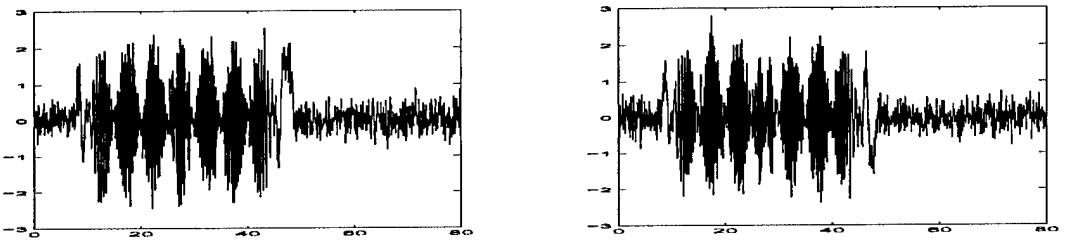

Real Imaginary

Figure 5.6. Zak transform of the sum of two shifted, noisy discrete chirps.

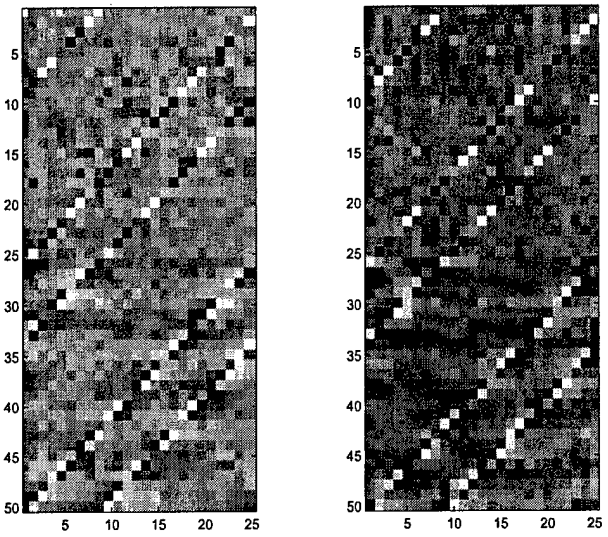

Real Imaginary

6 Windowing

Set

$$W_0 = \{(l,k) : 0 \leq l < L,\ 0 \leq k < K\}.$$

For $\mathbf{y} \in \mathbf{C}^{RN}$

$$W_0 P Z_{RL} \mathbf{y}$$

is the $L \times K$ image formed by restricting $PZ_{RL}\mathbf{y}$ to W_0. $W_0 P Z_{RL}\mathbf{y}$ is a view of $\mathbf{y}$ through the time-frequency window W_0.

The window W_0 results in local resolution by allowing the cyclic shift orthogonality of the discrete chirp to focus on N consecutive linear shifts of the corresponding zero-padded discrete chirp. Zak space formulation plays two roles, the design of the nonsingular discrete chirp satisfying the $L \times K$ Zak space condition and the viewing of the echo over a windowed

portion of the time-frequency Zak space. A future effort will include multiple Zak space dimensions and multiple chirp interrogations.

Algorithms to implement this are based on windowing the $RL \times K$ Zak transform of an echo $\mathbf{y}$. A more complex filtering of this Zak space image has also been developed. Surprisingly, perhaps, the resulting algorithm has simple structure. The range of applications is the same as that handled by the W_0-window algorithm. The eventual goal is to combine these approaches in a multiple chirp interrogation of a general target scene.

7 Zak Domain methods and Material Identification Algorithms

As with Zak space windows, future efforts will be directed to general Zak space filters, multiple chirp interrogations and the extensions of these methods to material identification. In particular, it is expected that the methods discovered thusfar in Phase III, combined with the material identification algorithms previously developed, will result in a refinement of these original algorithms.

Preliminary implementation of combining the material identification algorithms with Zak domain methods have been carried out. Starting with a sampled simulated echo, the decimation rate is determined by the chirp rate of the interrogating signal. Figures 7.7, 7.13 and 7.19 display the Zak domain images of echoes from several materials with varying delays.

Image processing methods in the Zak domain for denoising and focusing are under development. A two-step procedure of detection of lines using abelian group filters, followed by filtering in the image domain, has been implemented. Under an Air Force project (# F49620-98-C-0043), extensive research and development had been carried out for target detection/location. An internal development effort has produced a significant software toolbox for target detection/location. This toolbox has been used in an underwater mine detection problem. The combined research and application results are documented in [2]. We plan to use the full capability of the existing image processing software as well as tailoring the software for the Zak domain image processing for detection, location and denoising.

The following figures illustrate our preliminary investigations.

Figure 7.1. Zak transform of the sampled chirp, $\gamma = .125$, $T = 64$.

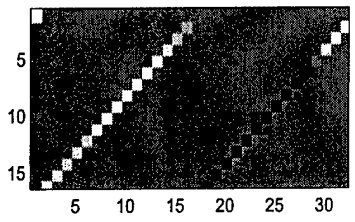

Real

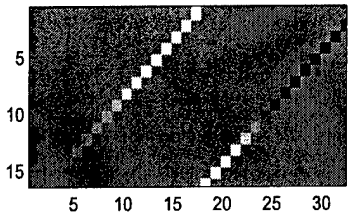

Imaginary

Figure 7.2. Test reflectivity kernel.

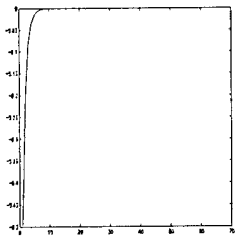

Figure 7.3. Received noise-free signal(echo), without delay.

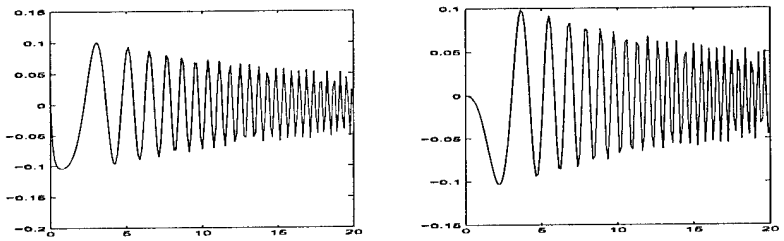

Real Imaginary

Figure 7.4. Received noisy signal(echo), with delay of 5 sample intervals.

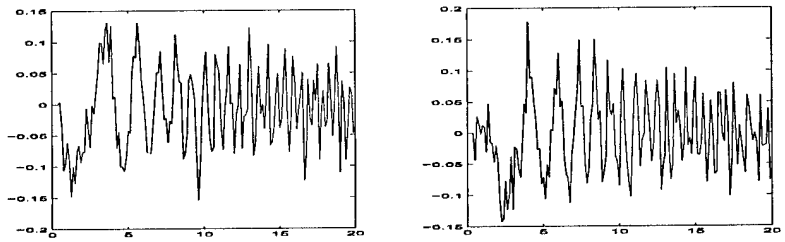

Real Imaginary

Figure 7.5. Auto-correlation of received, noisy signal with the transmitted chirp.

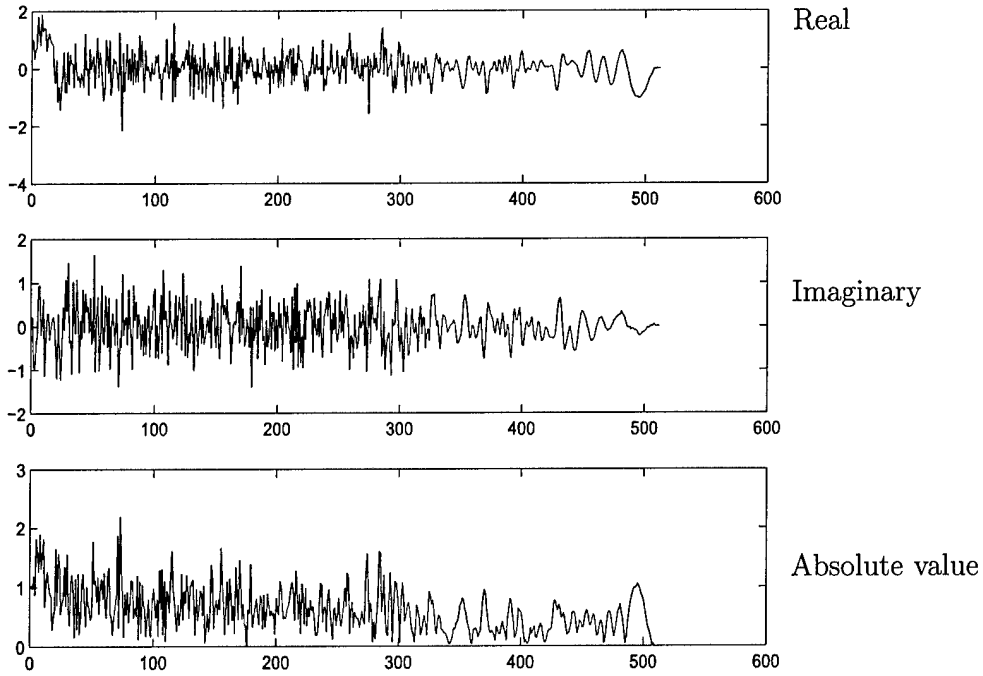

Figure 7.6. Zak transform of the noise-free echo, without delay.

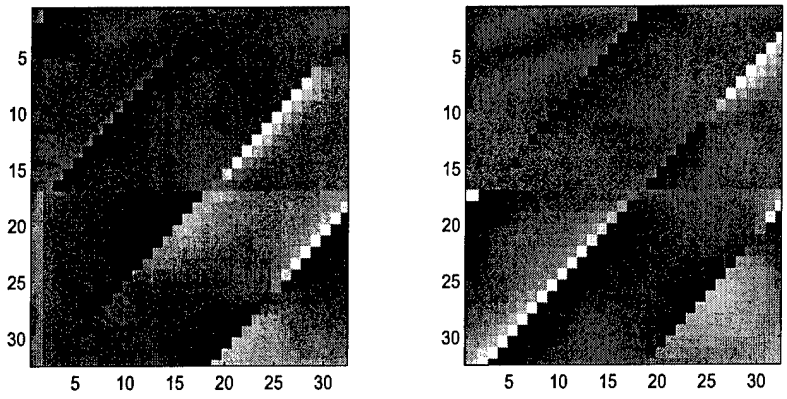

Figure 7.7. Zak transform of the noisy echo, with delay of 5 sample intervals.

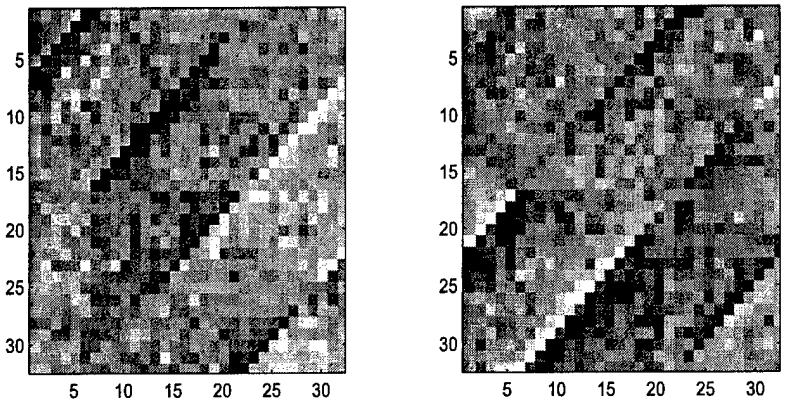

Figure 7.8. Test reflectivity kernel.

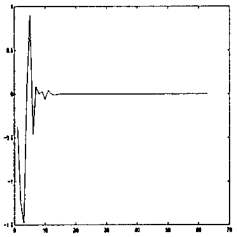

Figure 7.9. Received noise-free signal(echo), without delay.

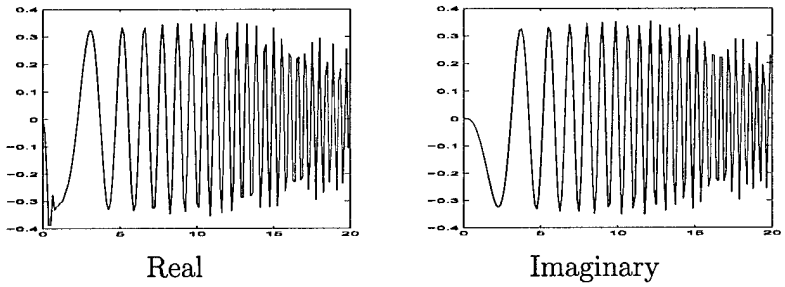

Figure 7.10. Received noisy signal(echo), with delay of 7 sample intervals.

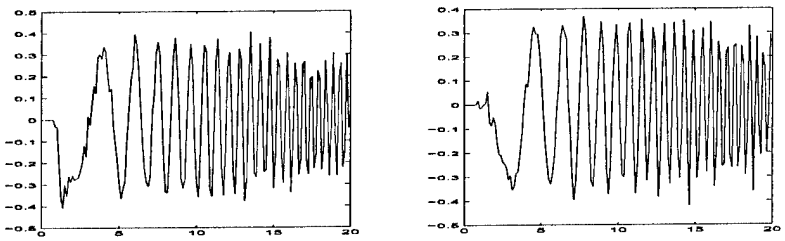

Real Imaginary

Figure 7.11. Auto-correlation of received, noisy signal with the transmitted chirp.

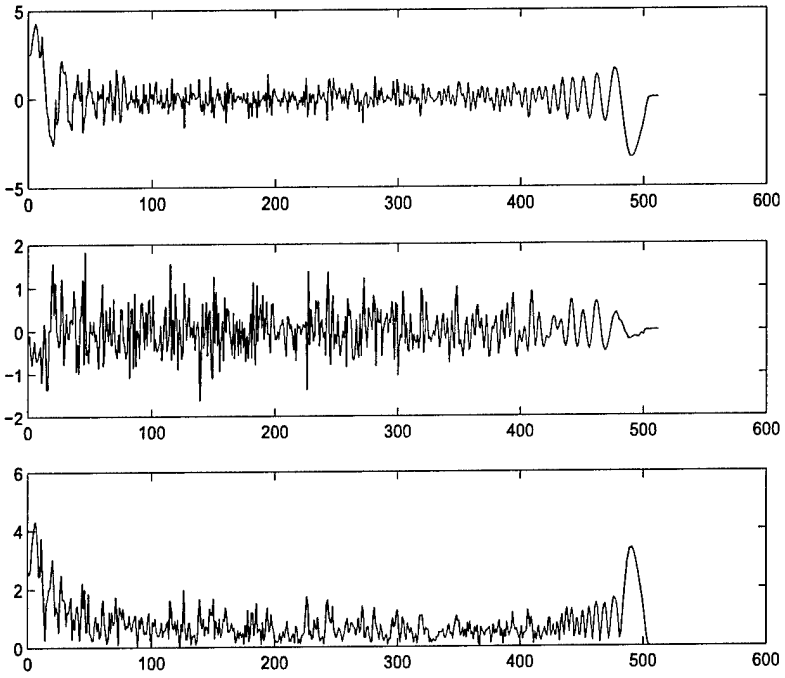

Figure 7.12. Zak transform of the noise-free echo, without delay.

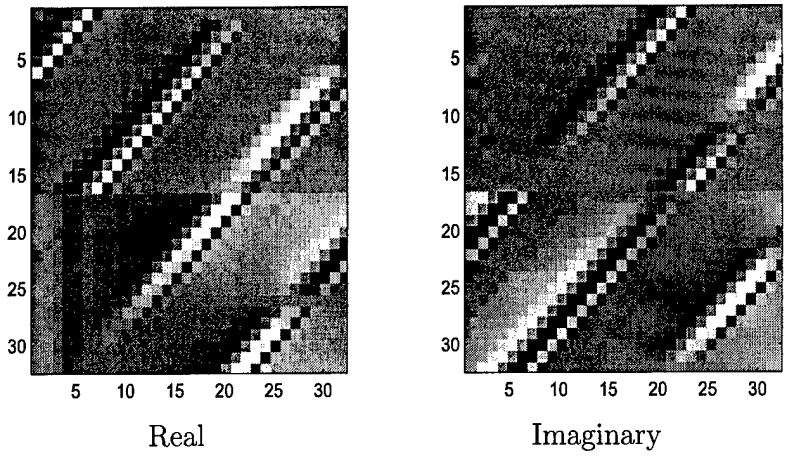

Figure 7.13. Zak transform of the noisy echo, with delay of 7 sample intervals.

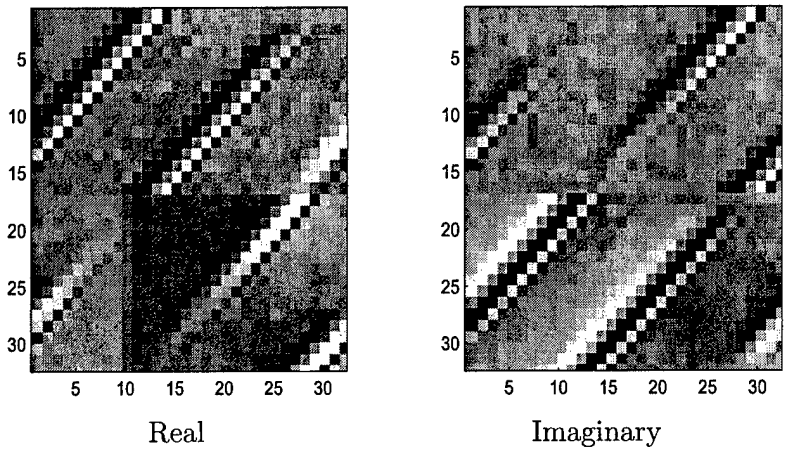

Figure 7.14. Test reflectivity kernel.

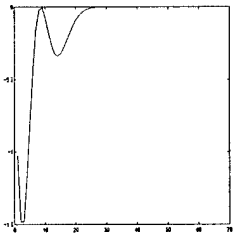

Figure 7.15. Received noise-free signal(echo), without delay.

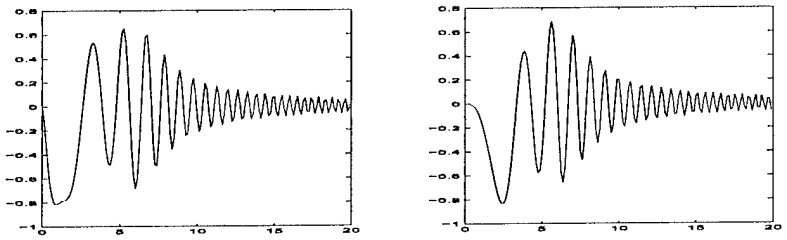

Figure 7.16. Received noisy signal(echo), with delay of 9 sample intervals.

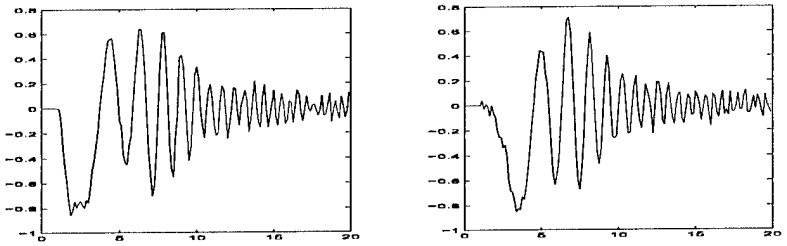

Figure 7.17. Auto-correlation of received, noisy signal with the transmitted chirp.

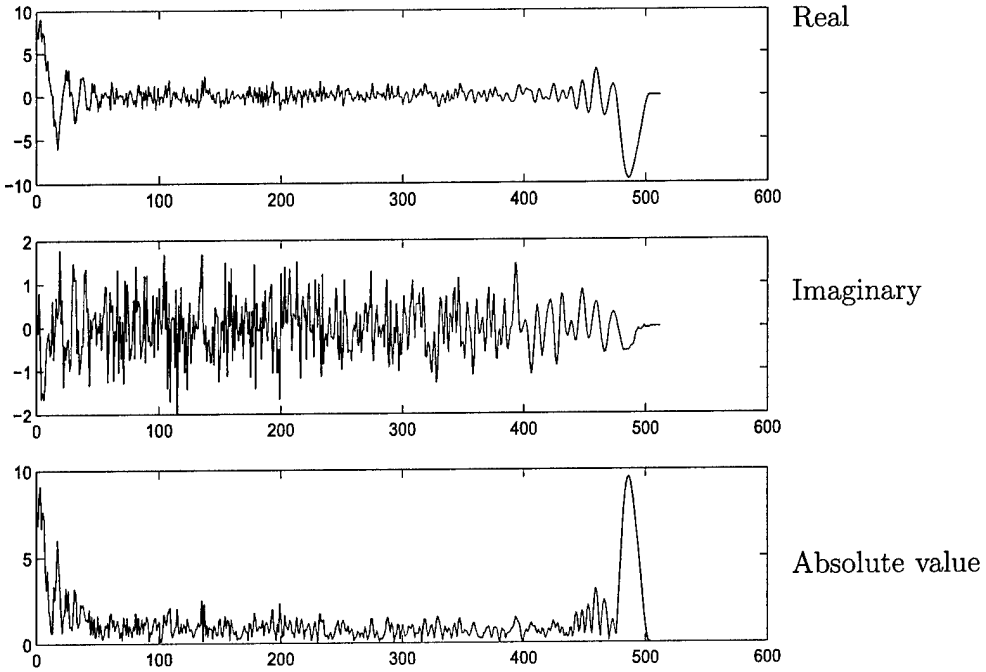

Figure 7.18. Zak transform of the noise-free echo, without delay.

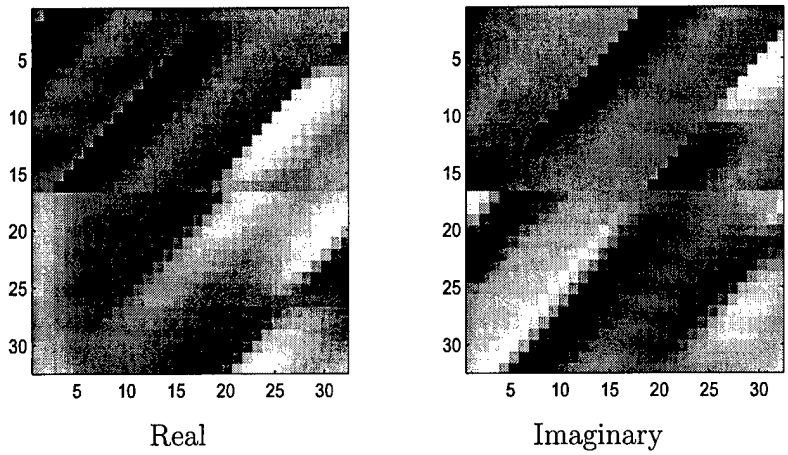

Figure 7.19. Zak transform of the noisy echo, with delay of 9 sample intervals.

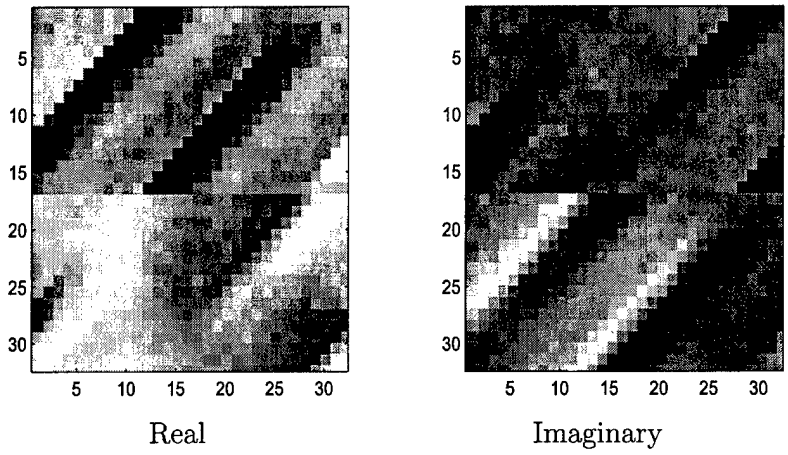

8 Future Efforts

While the current state of our theoretical and algorithmic results is sufficient for the solution of various important practical problems, many challenges remain. Our ultimate goal, which we believe is achievable within two years, is to combine Zak space windowing and filtering operations with multiple chirp interrogations for the purpose of designing robust and computationally efficient algorithms for resolving a general point target scene. We conclude by listing several steps, many of which will find immediate application when they are each achieved, that will enable this goal to be reached.

- For increasing target resolution, we will extend current results to apply to sample rates

which are any integer multiple of those given by the corresponding Zak space condition as well as samples at varying shifts.

Research is underway to characterize the collection of all discrete chirps satisfying this geometric Zak space property. The future effort will lead to greater flexibility as to acceptable sample rates for an analog chirp, acceptable meaning that the resulting sampled analog chirp and its echoes can be treated by the methods developed in this project. This effort will include multiple Zak space dimensions and multiple chirp interrogations.

- As with Zak space windows, future efforts will be directed to general Zak space filters, multiple chirp interrogations and the extensions of these methods to material identification. In particular, it is expected that the methods discovered thusfar in Phase III, combined with the material identification algorithms previously developed, will result in a refinement of these original algorithms.

- Two methods, windowing and filtering in Zak space, will be developed for removing the blurring in the Zak domain. Ultimately the underlying reason for being able to remove the blurring in this case is the local orthogonality of the discrete chirp x. Zak space provides the representation for implementing this time-frequency filtering.

- Image processing methods in the Zak domain for denoising and focusing are under development. A two-step procedure of detection of lines and partial lines using abelian group filters, followed by filtering in the image domain, has been implemented. More advanced noncommutative group filters are being tested to detect rotated and other corrupted lines.

  Several refinements to the current implementation are under development, including the use of noise characteristics. Once the location of lines is determined, the background (everything other than lines) will be characterized as noise. We will investigate methods of using this adaptive characterization to improve signal information.

- Chirps at different chirp rates have Zak space representations consisting of non-parallel lines. Since cross-correlations depend upon the intersections of shifts of these lines, they ought to be small. We will investigate the design of multiple-rate chirp sets solely by their Zak space representations to minimize cross-correlations in the context of waveform diverse SAR processing.

References

1. Phase II final technical report, contract # F33615–00–C–6012, 30 April, 2002.

2. Myoung An and Richard Tolimieri *Group Filters and Image Processing*, Psypher Press, 2003.

3. Richard Tolimieri and Myoung An, *Time-Frequency Representations*, Birkhauser, Boston 1998.

4. Richard Tolimieri, Myoung An and Chao Lu, *Algorithms for Fourier Transforms and Convolutions*, Springer-Verlag, 1997.